Journal of Statistical Physics, Vol. 107, Nos. 1/2, April 2002 (© 2002)

Towards a Renormalized Lattice Boltzmann Equation for Fluid Turbulence

S. Succi,[1] O. Filippova,[2] H. Chen,[3] and S. Orszag[4]

Received December 4, 2000; accepted October 10, 2001

A coarse-grained Lattice Boltzmann equation is examined in which the effects of unresolved (subgrid) scales are formally incorporated within a renormalized relaxation time of the collision operator. Actual values of the renormalized relaxation time are analyzed for the practical case of high-Reynolds flows past slant bodies (airfoils).

KEY WORDS: Lattice Boltzmann; renormalization group; multiscale computing.

1. INTRODUCTION

Lattice kinetic theory, and most notably the Lattice Boltzmann equation (LBE), have received considerable interest in the last decade as an efficient technique to compute a variety of fluid flows, ranging from low-Reynolds flows in porous media to highly turbulent flows in complex geometries.[(1–5)] The main assets of LBE are (i) mathematical simplicity, (ii) physical soundness and flexibility, (iii) computational efficiency especially on parallel computers. In a recent time, it has been argued that the above assets may turn even more valuable for the formulation of a renormalization-group treatment of fluid turbulence from the standpoint of kinetic theory.[(6)] This point of view is supported by mathematical and physical arguments, as well as by recent methodological advances in the field.

[1] Istituto Applicazioni Calcolo "M. Picone," Viale Policlinico 137, I-00161 Rome, Italy; e-mail: succi@iac.rm.cnr.it

[2] Institute of Combustion and Gas Dynamics, University of Duisburg, D-47048, Duisburg, Germany.

[3] EXA Corporation, Bedford Road 450, Lexington, Massachusetts 02420.

[4] Mathematics Department, Yale University, New Haven, Connecticut 06520.

0022-4715/02/0400-0261/0

The mathematical argument bears upon the simplicity of the formal structure of the Lattice Boltzmann equation: a linear streaming operator, as combined with a simple relaxation operator which encodes the entire non-linearity of the Navier–Stokes equations in a purely local form.

On a more physical ground, the idea is to revive the use of kinetic theory for the description of turbulent flows as a "gas of interacting eddies," along the spirit of the time-honored eddy-diffusivity theory. The challenge is to go beyond the standard low-Knudsen perturbative expansion which produces the Navier–Stokes equations out of the Boltzmann equation for real molecules, by means of a generalized LBE in which the non-perturbative interactions are lumped into an effective relaxation time scale in the LBE collision operator.

At the same time, the LB method has been enriched with multiscale, local-embedding capabilities, which extend its range of applicability to flow situations with sharp and localized features.[5, 7] For instance, multiscale LBE's have been recently applied to turbomachine flow calculations,[7, 8] and variable-grid-resolution commercial applications are now around for a number of years.[4]

In this paper, we introduce a renormalized Lattice Boltzmann equation and present preliminary multiscale LBE simulations which help assessing under which conditions coarse-graining of LBE may indeed contain additional information for the modeling and simulation of fluid turbulence in realistically complex geometries.

2. BASICS OF THE MULTISCALE LB METHOD

Multiscale Lattice Boltzmann schemes on Cartesian-like grids have been discussed in detail in several previous works, and therefore we shall present here only a cursory view of the basic elements. Our starting point is the lattice BGK formulation (LBGK) of fluid dynamics:[9]

$$f_i(\vec{x}+\vec{c}_i, t+1) - f_i(\vec{x}, t) = -\omega[f_i - f_i^e](\vec{x}, t) \tag{1}$$

where the time step has been made unity for simplicity. Here f_i is a set of discrete populations representing the probability of finding a particle at position $\vec{x}$ at time t moving along the direction identified by the discrete speed $\vec{c}_i$. The right hand side of (1) represents the relaxation to a local equilibrium f_i^e in a time lapse ω^{-1}. This local equilibrium is usually taken in the form of a quadratic expansion of a Maxwellian:

$$f_i^e = \rho w_i \left[1 + \frac{u_a c_{ia}}{c_s^2} + \frac{u_a u_b (c_{ia} c_{ib} - c_s^2 \delta_{ab})}{2c_s^4} \right] \tag{2}$$

where latin subscripts run over spatial dimensions, c_s is the sound speed and w_i is a set of weights normalized to unity. Once the discrete populations are known, fluid density and speed are obtained by (weighted) sums over the set of discrete speeds:

$$\rho = \sum_i f_i, \qquad \rho u_a = \sum_i f_i c_{ia} \tag{3}$$

The multiscale implementation of the LB method is based on the following steps. First, we perform a coarse-grain evolution (Collision + Streaming) step:

$$F'_i(\vec{X}, t) = (1-\Omega)\, F_i(\vec{X}, t) + \Omega F^e_i(\vec{X}, t) \tag{4}$$

$$F_i(\vec{X} + \vec{c}_i, t+1) = F'_i(\vec{X}, t) \tag{5}$$

where F is the coarse-grain distribution, $\vec{X}$ denotes a generic coarse node, $\vec{c}_i = n\vec{c}_i$ is the associated discrete speed (connectivity), n being the coarse-to-fine grid blocking/refinement factor, and Ω is the relaxation parameter in the coarse lattice. Finally, prime denotes post-collisional quantities. This provides all the populations in the coarse-grain nodes. Next we need to perform the fine-grain dynamics, actually n steps of size $\delta t = 1/n$ each, $t_k = t + k/n$, $k = 0, n-1$:

$$f'_i(\vec{x}_{m_1, m_2, m_3}, t_k) = (1-\omega)\, f_i(\vec{x}_{m_1, m_2, m_3}, t_k) + \omega f^e_i(\vec{x}_{m_1, m_2, m_3}, t_k)$$

$$f_i(\vec{x}_{m_1, m_2, m_3} + \vec{c}_i/n, t_k + 1/n) = f'_i(\vec{x}_{m_1, m_2, m_3}, t_k)$$

where $\vec{x}_{m_1, m_2, m_3} = \vec{X} + (m_1/n, m_2/n, m_3/n)$, $m_1 = 0,..., n-1$, $m_2 = 0,..., n-1$, $m_3 = 0,..., n-1$.

To ensure the same Reynolds number on both coarse and fine grids, the corresponding relaxation parameters must relate as follows:

$$\omega = \frac{\Omega/n}{1 + \dfrac{1-n}{n}\dfrac{\Omega}{2}} \tag{6}$$

Manifestly, $\Omega = \omega$ in the limit $n = 1$.

Therefore, n fine-grain steps complete the task of preparing for the next coarse-grain step.

Such a two-grid procedure must include a further rescaling operation in order to enforce fluxes continuity across the coarse-fine boundary. This crucial condition is secured by imposing the continuity of the first order non-equilibrium term $f^{ne}_i = f_i - f^e_i$ which, by virtue of (1), in the low-frequency limit simplifies to:

$$f^{ne}_i \sim -\omega^{-1} c_{ia} \partial_a f^e_i + O(Kn^2) \tag{7}$$

This leads to the following two scale transformations between the post-collisional coarse and fine-grain populations:

$$F'_i = F^e_i + (f'_i - f^e_i)\,\omega_{\text{eff}} \tag{8}$$

and

$$f'_i = f^e_i + (\hat{f}'_i - \hat{f}^e_i)\,\omega^{-1}_{\text{eff}} \tag{9}$$

where hat means interpolation from the coarse grid and

$$\omega_{\text{eff}} = n\,\frac{\omega(1-\Omega)}{\Omega(1-\omega)}$$

is the effective rescaled relaxation parameter.

Obviously, $f^e_i = F^e_i$ at the same node because the local equilibrium depends on the macroscopic properties of the fluid. Note that the transformations (8) and (9) reduce to identities in the limit $n \to 1$.

The final (pseudo)-algorithm reads as follows:

For $t = 0$, number of timesteps do:

1. Move and Collide F on the coarse grid
2. Scale F to f
3. For all subcycles $k = 0,\ldots, n-1$ do:
   (a) Interpolate F on the interface coarse-to-fine grid
   (b) Scale F to f via Eq. (9) on the interface coarse-to-fine grid
   (c) Move and Collide f on the fine grid

   End do subcycle
4. Scale back f to F via Eq. (8) on the interface fine-to-coarse grid

End do timesteps

Besides allowing selective grid refinements, typically around solid bodies, the previous procedure provides a potential operational candidate to test kinetic-based renormalisation-group formulations of fluid turbulence.[6]

3. TURBULENCE MODELING

Direct simulations of fluid turbulence are bound to be severely underresolved for many years to come, and consequently the problem of representing the effects of unresolved short-scales on the resolved ones (Large Eddies) remains key to both computational fluid dynamics and the theory

of turbulent flows. Mathematically, the problem of turbulence modeling is easily stated: find a functional correlation between the Reynolds stress tensor:

$$\sigma_{ab} \equiv \langle u'_a u'_b \rangle \tag{10}$$

and the resolved flow field U_a. In the above u'_a represents the sub-grid component of the flow field, e.g., the one fluctuating at scale shorter than the grid spacing. The simplest, and still very useful, type of correlation is based on the notion of eddy-diffusivity. The idea is that short-scale fluctuations respond linearly to the gradients of the resolved velocity field, the constant of proportionality being precisely the eddy diffusivity:

$$\sigma_{ab} = \nu_E S_{ab} \tag{11}$$

where

$$S_{ab} = \frac{\partial_a U_b + \partial_b U_a}{2} \tag{12}$$

is the resolved strain tensor. The eddy-diffusivity assumption is clearly borrowed from kinetic theory: a turbulent flow is likened to a gas of eddies, the smallest ones being enslaved to the local equilibrium generated by the large ones, and acting upon them like a diffusive process. It is also extremely convenient from the mathematical point of view, since it leaves the coarse-grained Navier–Stokes equations invariant, only with a renormalized, turbulent viscosity $\nu_T = \nu_E + \nu$. This analogy is inspiring, but often fails on quantitative grounds, basically because turbulent flows do not offer the type of scale separation between molecular and hydrodynamic scales which lies at the heart of kinetic approach to fluid dynamics. The whole field of turbulence modeling is devoted to the attempts to cope with this fundamental lack of scale separation. The simplest models just replace the constant ν_E with a local algebraic function of the (norm of) shear tensor S_{ab}. More sophisticated, and very popular models, let the eddy viscosity respond dynamically to the turbulent field by linking it to the actual values of the turbulent kinetic energy k and energy dissipation rate ϵ, via $\nu_E \sim k^2/\epsilon$, where k and ϵ evolve in time according to phenomenological transport equations.[10] More fundamental approaches, based on dynamic renormalization group (RG) techniques, derive such transport equations from recursive decimation of fast scales.[11] None of these approaches however proves capable of solving the turbulence modeling problem in full generality. It is therefore of interest to explore whether/what discrete kinetic theory can contribute to this complex scenario.

4. A REAL-SPACE RENORMALIZED LBE

In this section we shall discuss the potential of LBE for large-eddy simulation of fluid turbulence. The advocated assets of LBE for direct numerical simulations are:

- The streaming operator is linear
- The collision operator, which hides the entire non-linearity of fluid equations, is purely local in space

As observed in,[6, 12] these assets might even be furthered in the formulation of a renormalization-group approach based on kinetic theory rather than on continuum fluid equations. First, we observe that points 1 and 2 help taming one of the major hurdles of real-space renormalization, namely the proliferation of coupling constants from fine to coarse levels. Indeed, as we shall show shortly, the LBE formalism *naturally* conveys the effect of unresolved scales into a single scalar parameter, the renormalized relaxation frequency. Therefore, the renormalized LBE naturally preserves its invariance under the RG transformation. To illustrate the point, we shall refer to the continuum, differential form of LBE. Let us consider one step of the RG procedure.

First, rescale space-time by an infinitesimal amount: $\lambda = 1+\epsilon$, $\epsilon \ll 1$:

$$x \to \tilde{x} = \lambda x, \qquad t \to \tilde{t} = \lambda t, \qquad v = \tilde{v}, \qquad \tilde{f} = f \tag{13}$$

The transformed differential LBE $\lambda(\partial_{\tilde{t}} + \tilde{v}\partial_{\tilde{x}})\,\tilde{f} = -\omega[\tilde{f} - \tilde{g}]$ produces the trivial dimensional scaling $\tilde{\omega} = \omega/\lambda$. This simply means that in a lattice with λ times larger spacing, the relaxation frequency ω must be made λ times smaller to keep the same Reynolds number. Let us now interpret f in the LBE as the result of coarse graining over a finite volume of size h^{D+1}, where $h \equiv \Delta t$ and $c = 1$, so that $\Delta x = h$. This association is sound, since it is known that LBE can be obtained from the differential LBE by using a finite volume discretization with upwind interpolation and first-order time marching. In this case, the projector P_h from continuum to finite-scale h is simply a space-time integral over a 4-dimensional space-time cublet of size h:

$$f_h \equiv P_h f = \frac{1}{h^4} \int f \, d\vec{x}\, dt \tag{14}$$

It is clear that the space-time scaling can *not* leave the local equilibrium invariant because the quadratic dependence on f introduces subgrid

fluctuations $\langle f^2\rangle - \langle f\rangle^2$, where brackets stand for space-time integration over a 4-cublet of volume $(\lambda h)^4$. Let us first write:

$$f_i = g_i + f_i^{ne}$$

on the fine grid $h = 1$, where superscript *ne* denotes kinetic fluctuations at scale h and g_i is the local equilibrium at the same scale.

Coarse-graining with projector $P_{\lambda h}$ delivers:

$$\langle f_i\rangle = \langle g_i\rangle + \langle f_i^{ne}\rangle$$

which also rewrites as:

$$\langle f_i\rangle = g_i(\langle f_i\rangle) + \delta G_i + \langle f_i^{ne}\rangle$$

where the extra-contribution:

$$\delta G_i \equiv \langle g_i(f_i)\rangle - g_i(\langle f_i\rangle) \tag{15}$$

contains the *subgrid* fluctuations generated by the quadratic dependence of the local equilibrium on the local flow speed. From Eq. (2) we write explicitly

$$\delta G_i = \frac{\omega_i}{2c_s^4}\,(c_{ia}c_{ib} - c_s^2\delta_{ab})\,\sigma_{ab}$$

where σ_{ab} is the Reynolds stress tensor at scale λh, which includes all subgrid fluctuations within $[h, \lambda h]$ (denoted by tilde). With the notation: $F_i \equiv \langle f_i\rangle$ and $G_i \equiv g_i(\langle f_i\rangle)$, $F_i^{ne} \equiv F_i - G_i$, the coarse-grained LBE takes the form:

$$F_i(x+\lambda c_i, t+\lambda) - F_i(x,t) = -\frac{\omega}{\lambda}\,[F_i - G_i - \delta G_i]\,\lambda \tag{16}$$

The requirement of formal invariance of LBE under a complete renormalization cycle suggests to reabsorb subgrid fluctuations into a renormalized relaxation parameter $\omega(\lambda)$ such that the renormalized LBE takes the following final form:

$$F_i(x+\lambda c_i, t+\lambda) - F_i(x,t) = -\omega_i[\lambda][F_i - G_i]\,\lambda \tag{17}$$

where we have set:

$$\omega_i[\lambda] = \frac{\omega}{\lambda}\,(1 - s_i[\lambda]) \tag{18}$$

and

$$s_i[\lambda] \equiv \frac{\delta G_i(\lambda)}{F_i^{ne}(\lambda)} \tag{19}$$

This latter quantity represents the ratio of subgrid to kinetic fluctuations at scale λ, and formally collects *all* non-linear effects of subgrid physics. Neglect of these non-linearities would yield the trivial dimensional scaling $\omega(\lambda) = \omega/\lambda$.

From these definitions it is clear that sub-grid fluctuations are dynamically equivalent to kinetic fluctuations at scale λ.

The formal elegance of the renormalized LBE is apparent, and so is the transparence of its physical derivation. At no point did we have to assume that subgrid fluctuations (their variance) scale with the gradient of the resolved equilibrium, as typically required in a continuum approach in order to preserve functional invariance of the Navier–Stokes equation under coarse-graining. On the contrary, it is the mathematical LBE formulation itself that conveys subgrid contributions into a renormalized frequency in a very natural way.

Of course, the question is: *what new insights are to be expected from the renormalized LBGK as compared to the Navier–Stokes picture*?

Apparently, not much at all, since we are still left with the usual problem of expressing the Reynolds stress tensor as a function(al) of the resolved field. However, a slightly deeper thought reveals that *the renormalized LBE might not converge to the corresponding coarse-grained Navier–Stokes equations*, because the assumption of small mean-free path (low Knudsen number) might break-down at the coarser levels of the coarse-graining procedure.

Symbolically:

$$\langle LBE \rangle = \langle NSE \rangle + HOT \tag{20}$$

where brackets stand for coarse-graining and HOT means higher-order-terms associated with non-adiabatic departures from local equilibrium (which are by definition negligible at the finest scales, where it is understood that LBE is equivalent to the Navier–Stokes equations). Of course, there is no guarantee that HOT correctly describes the physics of turbulent fluctuations. However, we are least guaranteed that the equation (17) contains a fully non-perturbative resummation of an infinite series of diagrams associated with non-small Knudsen numbers, while it is well known that any finite expansion beyond second order (Navier–Stokes) in terms of differential operators is doomed to instability. In view of the lack of scale

separation discussed previously, it seems therefore that RGLBE provides a reasonable starting point in the direction of trying to go beyond eddy-diffusivity models of fluid turbulence.

4.1. Analysis of the Renormalized LBE

To analyse the qualitative scenarios associated with the renormalized LBE it is convenient to recast the relation (18) in terms of a corresponding renormalized relaxation time:

$$\tau(\lambda) = \frac{\lambda\tau(1)}{1-s(\lambda)} \tag{21}$$

with the obvious condition $s(1) = 0$.

Three characteristic regions stand out:

1. $s < 0$,
2. $0 < s < 1$
3. $s > 1$

Let us for simplicity refer to the case in which F_i relaxes to its local equilibrium G_i from above (see Fig. 1).

In terms of local relaxation, the condition $s < 0$ means that subgrid fluctuations move the renormalized equilibrium:

$$F_i^e \equiv G_i + \delta G_i$$

farther apart from F_i as compared to the bare equilibrium G_i. The first region is therefore characterized by a decreasing effective relaxation time, hence increasing effective Reynolds number, at large scales. This is *not* expected to be the case for turbulent flows in which small eddies are known to relax faster than large ones.

The second region is characterized by the opposite behaviour: the subgrid fluctuations take the renormalized equilibrium closer to F_i. This corresponds to an increasing effective relaxation time, so that the effective Reynolds number becomes smaller and smaller at large scales, This is the standard infrared-free scenario in which the renormalisation procedure is expected to apply. Within this region, we recognize that the relaxation time may eventualy get so high that the corresponding mean-free path of the small eddies may no longer be small enough to justify the assumption of small departures from local equilibrium around large ones. This is potentially the most interesting region for LBE-based turbulence models, since it

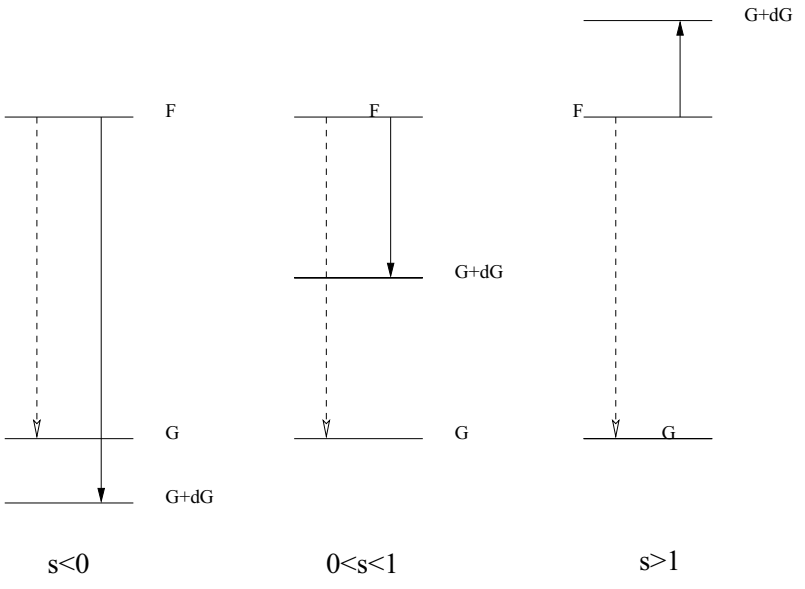

Fig. 1. Schematic view of the bare (dashes) and renormalized (solid) relaxation process for the three cases $s < 0$, $0 < s < 1$, and $s > 1$ respectively.

is here that the additional information associated with the renormalized LBE—if any—must reside.

Finally, the third region marks situations in which coarse-graining fluctuations are strong to the point of driving the viscosity formally negative, through a sort of "phase-transition". The physical meaning of this negative viscosity as follows. What the condition $s > 1$ means is that the renormalized equilibrium F_i^e "overshoots" the actual value of F_i so that effective relaxation takes place along the opposite direction (growing F_i) as compared to bare relaxation. This scenario is physically associated with violent bursts and local instabilities. It is probably a desirable feature for the effective viscosity to be occasionally allowed to decrease, and even become negative, under coarse-graining, for this provides the potential capability of capturing the effects of the aforementioned instabilities for the important case of transitional turbulence. Of course, the practical issue of numerical stability in this third region remains entirely open.

This completes the qualitative analysis of the renormalized LBE.

It is clear that the practical value of the renormalized LBE hings critically on the possibility of deriving a concrete expression for the effective relaxation parameter as a functional of the resolved flow field. We shall return to this point shortly.

5. PRELIMINARY TESTS: FLOW PAST AN AIRFOIL

The above ideas have been tested on a two-dimensional flow of practical interest, using a multiscale LBE code with local grid-refinement capabilities. Before plugging back into the renormalization issues, we provide some details of preliminary validation tests.

5.1. Validation Tests

As a preliminary testbed for the ideas discussed above, we have validated the multiscale method through a series of numerical simulations of a vortical flow around an airfoil in cascade at $Re = 5000$ and angle of attack $\alpha = 20°$. The geometry of the cascade is described in details in ref. 13. Flows around airfoils at high Reynolds numbers contain regions of large gradients in some localized zones of the curvilinear boundaries (e.g., in the vicinities of the leading or trailing edge of an airfoil). Therefore here we resolve the flow around an airfoil on a set of multiple embedded grids. Multiple embedding means further local refinement of previously refined grids. The interface conditions[5] in the case of a crossing boundary are extended by linear interpolation of the post-collision distribution functions from the "fluid" to the "rigid" nodes of the coarse-to-fine grid interface. Boundary-fitting formulas for no-slip conditions on the surface of the airfoil are applied in all nodes neighbouring to the boundary on the finest grid in this region.

For the validation of the results obtained with the multiscale LBGK code the same flow is computed with the commercial CFD code FLUENT 5 using constant density. The basic hybrid grid A (20997 nodes, grid generator GAMBIT) is shown in Figs. 2a and 2b. To provide the finer spatial resolution in the regions of larger gradients the basic grid A is refined in the vicinity of an airfoil by factor 2 (grid B, 65368 nodes, Fig. 2c). Computations with the multiscale LBGK code are performed on the set of embedded grids G_1, G_2, G_3, G_4. Their relative positions in the vicinity of an airfoil are shown in Fig. 2d. The coarsest grid G_1 covering the whole computational cell consists of 350×81 nodes. In addition the instantaneous streamlines of the flow in periodical regime are shown in Fig. 2d.

At first, the solution obtained with the multiscale LBGK scheme on the set of multiple embedded grids G_1, G_2, G_3, G_4 with refinement ratio 8:2:1:1 and $M_{num} = 0.09$ is compared with those obtained with FLUENT 5. The curves of the lift coefficients C_L corresponding to the forces acting perpendicular to the chord of the airfoil are plotted in Figs. 3a and 3b. The results obtained with FLUENT 5 are shown in Figs. 3a and 3b with dotted curves. The curves are marked with alphabetic characters defining a hybrid

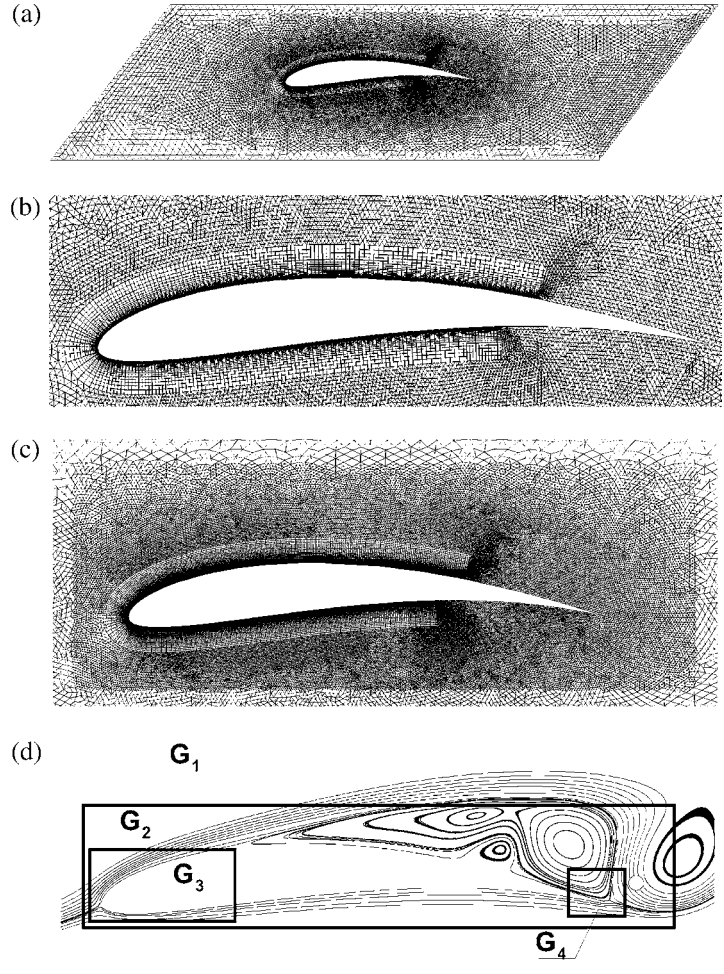

Fig. 2. (a) hybrid grid A used in the numerical simulations with FLUENT 5 in the whole computational cell. (b) Enlarged part of the grid A in the vicinity of an airfoil. (c) Enlarged part of the grid B in the vicinity of an airfoil. (d) Boundaries of embedded Cartesian grids G_2, G_3, G_4 used in the numerical simulations with the multiscale LBGK code; instantaneous streamlines in the vicinity of an airfoil in periodical regime.

grid used in the computations (A or B). Time-stepping is marked on all curves with solid circles.

The unsteady solver in FLUENT 5 is implicit and segregated with SIMPLE pressure-velocity coupling. Under-relaxation factors in pressure and momentum equations are chosen as 0.3, 0.8.

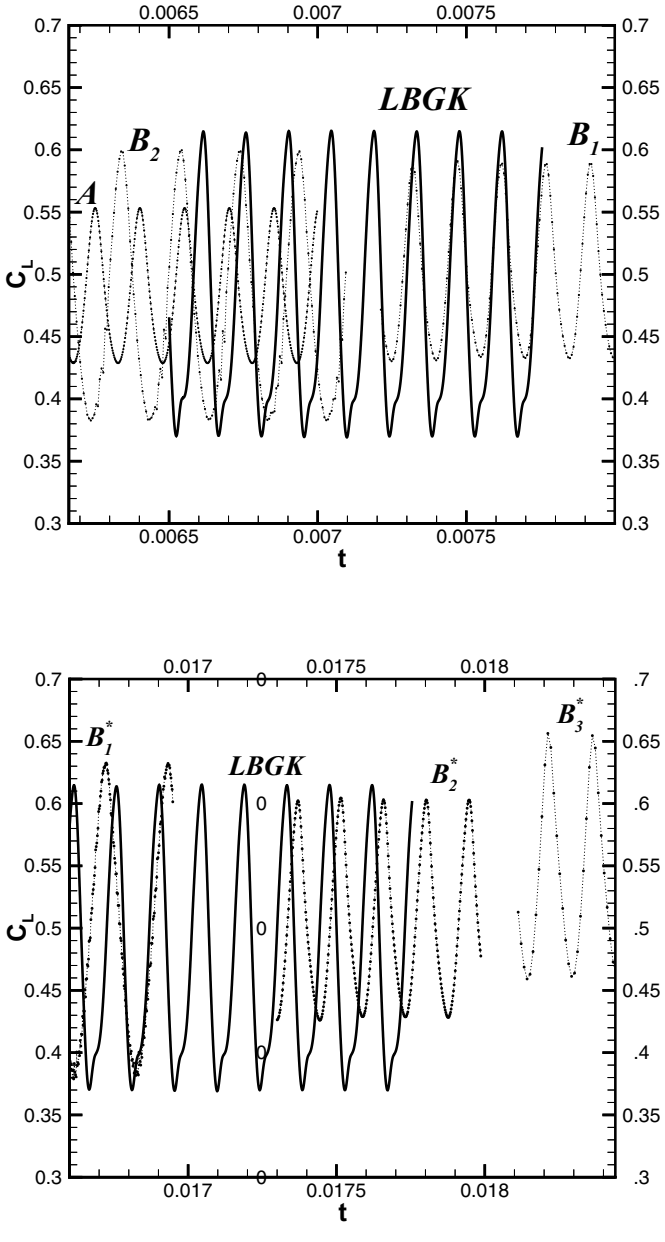

Fig. 3. Unsteady periodical flow around an airfoil in cascade at $Re = 5000, \alpha = 20^o$. Temporal development of the lift coefficient obtained with the multiscale LBGK code on the set of multiple embedded grids G_1, G_2, G_3, G_4 with refinement ratio 8:2:1:1 and FLUENT 5.

In the simulations shown in Fig. 3a a second order accurate in time solver is used with the default spatial discretization: second order accurate for viscous terms and first order upwind for convection terms in governing equations. Different convergence criteria, based on the values of residuals in continuity and momentum equations, are used in the simulations presented in Fig. 3a: $1 \cdot 10^{-4}$ for curves A, B_1 and $5 \cdot 10^{-3}$ for curve B_2.

In Fig. 3b the results of the computations with second order accurate in space solver on grid B are presented, whereas the accuracy in time is varied from first order (Fig. 3b, curves B_1^*, B_2^*) to second order (Fig. 3b, curve B_3^*). Different convergence criteria based on the values of residuals in continuity and momentum equations are used in the simulations presented in Fig. 3b: $5 \cdot 10^{-3}$ for curve B_1^* and $1 \cdot 10^{-3}$ for curve B_2^*, B_3^*.

We wish to emphasize that during the iterations residuals in momentum equations decrease faster than the residual in continuity equation, so the convergence criterion in our simulations with FLUENT 5 is defined virtually by the value of the residual in continuity equation.

Figures 3a and 3b show that the averaged values of the lift coefficients obtained with FLUENT 5 on grids A, B are in the good agreement. The amplitude of the oscillations of the lift coefficient C_L and the frequency of the flow obtained with FLUENT 5 depends on the spatial and temporal resolution and convergence criterion and vary in order of 10% in our simulations. This sensitivity of time-dependent wake flows behind airfoils to numerical influences, even in the range of the truncation error, was found also in ref. 13.

As one can see from Figs. 3a and 3b the solution obtained with the multiscale LBGK scheme is well within the sensitivity range of the conventional CFD solver for time-dependent incompressible flows.

In addition the grid resolution study of the results obtained with the multiscale LBGK solver was performed. The results for the lift coefficients obtained on the set of multiple embedded grids G_1, G_2, G_3, G_4 with refinement ratio 12:2:1:1 and 8:2:1:1 are shown in Fig. 4. The values of the relaxation parameters on grids $G_2 - G_4$ are $\omega_{G_2} = 1.863$, $\omega_{G_3} = \omega_{G_4} = 1.744$ for refinement ratio 12:2:1:1 and $\omega_{G_2} = 1.907$, $\omega_{G_3} = \omega_{G_4} = 1.822$ for refinement ratio 8:2:1:1. On the coarse grid G_1, where the flow can be considered as inviscid, an artificial value of the relaxation parameter $\omega_{G_1} = 1.85$ instead of the "right" value $\omega_{G_1} = 1.976$ was used according to the concept of artificial viscosity for inviscid flow simulations.[8]

5.2. Monitoring LBE Subgrid Fluctuations

To assess the nature of subgrid fluctuations and the high-Knudsen issue discussed previously, we monitor the kinetic and subgrid fluctuations

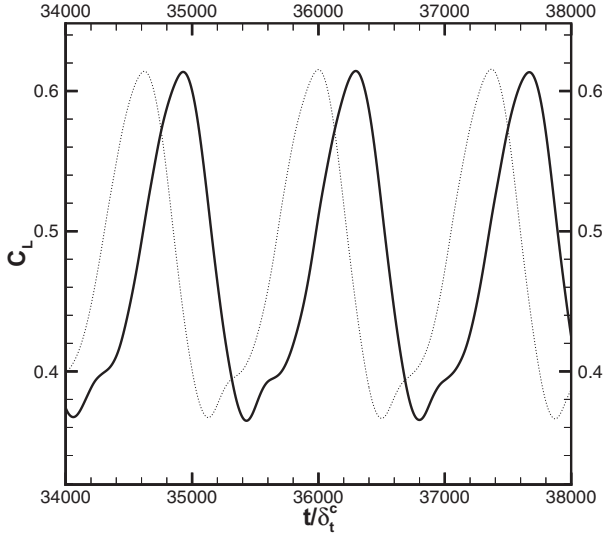

Fig. 4. Unsteady periodical flow around an airfoil in cascade at $Re = 5000, \alpha = 20°$. Temporal developmemt of the lift coefficient obtained with the multiscale LBGK code on the set of multiple embedded grids G_1, G_2, G_3, G_4 with refinement ratio 12:2:1:1 (bold solid lines) and 8:2:1:1 (dotted lines).

at a given spatial location, marked in Fig. 2d with solid circle. The visualisation of the flow confirms that the reference point is chosen in the zone of the vortex shedding. At this spatial location we measure both the ratio s of subgrid to kinetic fluctuations, and the coarse-grained "Knudsen number" defined as:

$$K_i \equiv \frac{F_i - G_i}{F_i}$$

With this definition, the total kinetic + subgrid relative departure at scale λ ("turbulent Knudsen number") is given by:

$$K_i(s) \equiv \frac{F_i - G_i - \delta G_i}{F_i} = K_i(1 - s_i)$$

For simplicity, we confine our attention to north-east propagating distributions, f_2, whose non-equilibrium components respond to transverse shear components.

In Figs. 5a and 5b we show s_2 as measured at two distinct coarse-graining scales, $\lambda = 3$ and $\lambda = 11$. From these figures we see that $s(\lambda)$ grows more than linearly with the size of the averaging box and attains values within the range $[0, 1]$ the region, as expected. With $\lambda = 11$, we measure a maximum around $s \sim 0.6$, which corresponds to an enhanced relaxation $\tau(11)/11\tau(1) \sim 10/4 = 2.5$, hence only moderately higher than the purely dimensional value. Given that the bare value of $11\tau(1) \sim 0.012$, the renormalized relaxation time $\tau(11) \sim 0.03$ is still small enough to justify the hydrodynamic limit also at the coarsest scale.

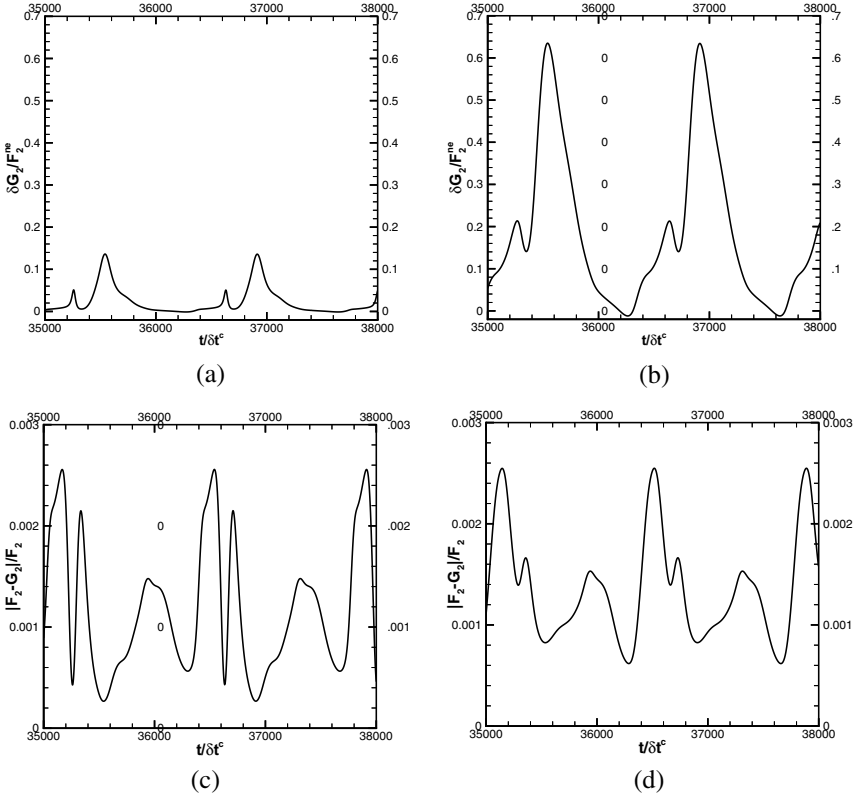

Fig. 5. Unsteady periodical flow around an airfoil in cascade at $Re = 5000, \alpha = 20°$. (a) Temporal development of $\delta G_2/F_2^{ne}$ in the reference point, $\lambda = 3$. (b) Temporal development of $\delta G_2/F_2^{ne}$ in the reference point, $\lambda = 11$. (c) Temporal development of $|F_2 - G_2|/F_2$ in the reference point, $\lambda = 3$, $p_{outlet}/c_s^2 = 3$. (d) Temporal development of $|F_2 - G_2|/F_2$ in the reference point, $\lambda = 11$, $p_{outlet}/c_s^2 = 3$.

The time evolution of the turbulent Knudsen number is displayed in Figs. 5c and 5d. From these figures, we see that indeed $K \ll 1$ and remains almost the same on both coarse-grained grids. We conclude that, for the present flow, the renormalized LBE is not expected to contain any significant information as compared with the coarse-grained Navier–Stokes equations.

The above conclusions might well change for highly turbulent flows in which stronger fluctuations are expected to populate the region in the vicinity of $s = 1$.

5.3. Native Kinetic-Theoretical Turbulence Models

Monitoring the high-Knudsen issue in coarse-grained LBE simulations is important since it sheds light into the critical question of whether coarse-grained kinetic theory can yield additional information as compared to coarse-grained fluid-dynamics. However, it can hardly provide an operational input to the problem of turbulence modeling.

To this purpose, one has to link the renormalized relaxation time to coarse-grained observables. A practical strategy (we are indebted to Dr. V. Yakhot for clarifying this point)[14] is to express the effective relaxation time in the form of a semi-empirical functional of the main turbulent observables

$$\tau = \frac{k}{\epsilon} \Psi(\eta) \tag{22}$$

where k is the turbulent kinetic energy, ϵ the turbulent energy dissipation, τ_0 the bare relaxation time and $\eta = \tau_0 |S|$ a dimensionless strain parameter measuring the departure of turbulent fluctuations from local equilibrium.

By definition, Ψ is significantly different from unit value only in regions where turbulence is highly off-equilibrium (typically near-wall regions), while away from these regions $\Psi(\eta) = 1$, corresponding to the standard k–ϵ model. Once a given $\Psi(\eta)$ is specified, the effective relaxation time can be updated self-consistently by coupling LBE with allied dynamical equations for k and ϵ. It should by now be clear that specifying a self-consistent relaxation time goes in principle beyond effective-viscosity representations because the renormalized LBE contains corrections to *all orders* in the "turbulent" Knudsen number.

This type of simulations, with $\Psi = 1$, (standard k–ϵ turbulence model) have been recently performed with satisfactory results.[8] Of course many issues still need further exploration, for instance the symmetry requirements on the set of discrete speeds in order to ensure the correct representation

of the higher order terms.[15] Going beyond these LBGK-k–ϵ turbulence models represents, in our opinion, one of the most tantalizing directions of future Lattice Boltzmann research.

ACKNOWLEDGMENTS

Work partly performed under the NSF grant "Kinetic Theory method for Large-Eddy Simulation of Turbulence," (DMS-9974289) at Yale University. Useful discussions with Prof. V. Yakhot are kindly acknowledged.

REFERENCES

1. R. Benzi, S. Succi, and M. Vergassola, *Phys. Rep.* **222**:145–197 (1992).
2. S. Chen and G. D. Doolen, *Ann. Rev. of Fluid Mech.* **30**:329 (1998).
3. S. Succi, *The Lattice Boltzmann Equation* (Oxford University Press, 2001).
4. H. Chen, C. Teixeira, and K. Molvig, *Int. J. Mod. Phys C* **8**:675 (1997).
5. O. Filippova and D. Hänel, *J. Comp. Phys.* **147**:219–238 (1998).
6. H. Chen, S. Succi, and S. Orszag, *Phys. Rev. E* **59**(3):R2527 (1999).
7. F. Mazzocco, W. Arrighetti, G. Bella, L. Spagnoli, and S. Succi, *Int. J. Mod. Phys. C* **11**(2):233 (2000).
8. O. Filippova, S. Succi, F. Mazzocco, C. Arrighetti, G. Bella, and D. Hänel, *J. Comput. Phys.* **170**:812 (2001).
9. Y. H. Qian, D. d'Humieres, and P. Lallemand, *Europhys. Lett.* **17**(6):479–484 (1992).
10. B. Launder, *Simulation and Modeling of Turbulent Flows*, T. Gatski, M. Hussaini, and J. Lumley, eds., ICASE/Larc Series in Computational Science and Engineering, Vol. 109 (Oxford University Press, 1996).
11. V. Yakhot and S. Orszag, *Phys. Rev. Lett.* **57**:1722 (1986); *J. Sci. Comp.* **1**:3 (1986).
12. S. Succi, H. Chen, I. Karlin, and S. Orszag, *Physica A* **280**:92 (2000).
13. O. Filippova and D. Hänel, *J. Comput. Phys.* **165**:407 (2000).
14. C. Alexander, *et al.*, Turbulent flow simulations via extended lattice Boltzmann algorithm, EXA preprint 2001; V. Yakhot *et al.*, A new approach to modelling strongly non-equilibrium, time-dependent, turbulent flows, EXA preprint 2001; R. Shock *et al.*, Recent simulation results on 2D NACA airfoils using Lattice-Boltzmann based algorithm, EXA preprint 2001.
15. M. Vergassola, R. Benzi, and S. Succi, *Europhys. Lett.* **13**(8):727 (1990).